Lipoblastoma in one adult and 35 pediatric patients: Retrospective analysis of 36 cases

WENCHUAN ZHANG, SHUWAN ZHANG, ZIXIN YANG, YING ZHANG and ZHE WANG

Department of Pathology, Shengjing Hospital of China Medical University, Shenyang, Liaoning 110004, P.R. China

Received July 17, 2022; Accepted October 17, 2022

DOI: 10.3892/etm.2022.11710

Abstract. Lipoblastoma is a rare benign mesenchymal neoplasm that typically occurs at various sites in infants and children but may also occur in adults. Thus, differential diagnoses are often performed. To understand this tumor type, the present study described clinicopathological features, diagnosis and differential diagnosis of different morphological lipoblastomas. A single-institution retrospective review of 36 lipoblastoma cases diagnosed between 2015 and 2021 was performed. Formalin-fixed paraffin-embedded tissue was used for S-100, CD34, P16 and desmin immunohistochemistry analysis, along with rapid fluorescence *in situ* hybridization (FISH) detection with pleiomorphic adenoma gene 1 (*PLAG1*). The 36 cases included 14 females and 22 males [age range, 7 days to 33 years (median, 16.5 years); 28 patients were aged ≤3 years] and the tumors were located in the trunk (n=16), limbs (n=12), head and neck (n=6), and perineum (n=2). Histologically, lipoblastomas were divided into classic (n=15), lipoma-like (n=13) and myxoid (n=8) subtypes. They comprised lobules of mature adipose tissue of varying size and a fine capillary network surrounded by mucinous stroma. Single- or multivesicular lipoblasts positive for S-100 (29/36, 81%) were observed, with occasional mature adipocytes. Peripheral vessels and cytoplasm of primitive mesenchymal cells were diffusely positive for CD34 (36/36, 100%), whereas primitive mesenchymal cells and striated muscle tissue were positive for desmin (26/36, 72%). Most tumor cells were negative while only few were positive for P16 (8/36, 22%). FISH revealed *PLAG1* breakage and rearrangement in 24/32 (75%) patients. In total, 28 patients were followed up post-operatively (range, 2-84 months; median, 41 months; 3 patients relapsed and 8 were lost to follow-up). In conclusion, diagnosis of a typical lipoblastoma is not difficult and *PLAG1* breakage detection is key for the diagnosis.

Correspondence to: Professor Zhe Wang, Department of Pathology, Shengjing Hospital of China Medical University, 36 Sanhao Street, Shenyang, Liaoning 110004, P.R. China
E-mail: wz_cmu@126.com

Key words: lipoblastoma, fusion gene, *PLAG1*, differential diagnosis, neoplasm

Introduction

Lipoblastoma is a benign tumor of the embryonic white fat with a prevalence of ~0.6% of benign soft tissue tumors (1). It is the second most common childhood adipocyte tumor after lipoma and typically occurs in boys younger than three years of age (2,3). Lipoblastomas are often present in the extremities, trunk and head and neck, but they may also appear in the mediastinum, retroperitoneum, perineum and parotid gland (4). Most lipoblastomas are ≤5 cm in size, but larger sizes occasionally occur. Magnetic resonance imaging is the preferred modality for assessing tumor location, size, composition, adjacent organs and surgical resection site (5). Although preoperative imaging is useful in assessing the extent of the tumor, it cannot differentiate between various adipose tissue tumors because there are no pathological imaging features associated with lipoblastoma (6). Treatment typically involves complete surgical removal and preservation of the vital organs. The disease is a benign lesion with a good prognosis, with no reports of malignant transformation and metastasis. Although there is no risk of metastasis, it may relapse in the late stage with incomplete resection (1).

Lipoblastomas typically exhibit a simple pseudodiploid or hyperdiploid karyotype. The most common type is one or more additional copies of chromosome 8, which contains structural abnormalities at 8q11-13 (including translocation, insertion, inversion, or circular chromosomes), resulting in pleiomorphic adenoma gene 1 (*PLAG1*) rearrangement (2).

PLAG1 is primarily composed of five exons, and codes from exon 4 produce a protein composed of 500 amino acids. Its oncogenic effect is associated with upregulation of multiple direct target genes, including growth factors, growth factor-binding proteins, growth factor receptors and cell cycle-associated proteins, such as insulin-like growth factor 2, vascular endothelial growth factor and mitogen-activated protein kinase (7-11). *PLAG1* acts as a transcriptional regulator and is not expressed in adult tissue (12,13). It is hypothesized that this is due to the presence of negative control elements that inhibit PLAG gene expression) in exon 1 of *PLAG1* in adults; however, ectopic *PLAG1* in tumors results in loss of these elements and overexpression of the coding region (14). Tumors caused by overexpression of *PLAG1* include salivary gland pleomorphic adenoma, lipoblastoma, hepatoblastoma and acute myeloid leukemia (15). Detection of *PLAG1* rearrangement is helpful in the diagnosis of pleomorphic adenoma. Andreasen *et al* (16) found that 16 (76.2%) of 21 pleomorphic

adenomas showed copy-neutral *PLAG1* rearrangements. Four other markers also serve a role in the development of lipoblastoma including CD34, S-100, desmin, and p16. It has been reported that the $CD34^+$ fibroblastic stem cell may be the putative cell of origin for lipoblastoma (17). S-100-positive mono- and multi-vacuolar lipoblasts indicate tumor origin in adipose tissue (18). Aberrant immunoreactivity to desmin has been described in non-adipose mesenchymal tumors, except those with myogenic or myofibroblast differentiation (17,19). In the study by Kubota *et al* (20), PLAG1-positive spindle cells expressed desmin, but not other myogenic markers. Combining the immunological features of desmin, spindle cell morphology and ultrastructural features (invaginated nuclei, well-developed rough endoplasmic reticula, pinocytotic vesicles and desmin filaments), it was inferred that spindle cells in lipoblastoma may exhibit myofibroblastic differentiation. *PLAG1* overexpression and activation are key events in lipoblastoma and this pathway is independent of p16. However, alterations in the retinoblastoma pathway during liposarcoma development serve a key role in overexpression of p16 (21,22). P16 immunohistochemistry has been reported to show high negative predictive value from lipoblastoma (87%) and benign adipocytic lesions (93%) in differentiating liposarcoma (23,24). Therefore, malignancy is unlikely in the absence of p16 expression.

Morphologically, lipoblastoma is primarily composed of primitive spindle mesenchymal cells and adipocytes at various stages of maturation. In particular, it contains lobules of mature adipocytes of different sizes divided by fiber septa, with a fine capillary network and mucinous stroma. In immunohistochemistry, lipoblasts are usually S-100-positive and P16-negative, while CD34 and desmin expression is usually observed in primitive mesenchymal cells; these properties serve as a useful diagnostic marker (20,25). However, because lipoblastoma has its own characteristic genetic changes, fluorescence *in situ* hybridization (FISH) detection of *PLAG1* fragmentation and rearrangement may be useful in diagnosis of lipoblastoma (26,27).

Furthermore, lipoblastoma often shows atypical morphology or occur in young and adult age groups and are easily misdiagnosed as lipoma, fibrous hamartoma of infancy, myxoid liposarcoma, primitive myxoid mesenchymal tumor of infancy and superficial angiomyxoma (28-30). Therefore, as a cytogenetic detection method, *PLAG1* FISH is required to aid the diagnosis by pathologists. Currently, reports on this disease are mostly limited to case reports (4,5,8,26). Therefore, to gain a deeper understanding of the occurrence and development of lipoblastoma, changes in molecular structure and the effect of fusion genes on prognosis, the present study collected 36 cases of lipoblastoma in Shengjing Hospital of China Medical University over the past 7 years. Combined with evidence from international literature (1,3-6,8,17-20,25,26), the present study summarized clinical features, morphological changes, immunophenotype, FISH detection, diagnosis and differential diagnosis, to improve the accuracy of diagnosis and decrease the rate of misdiagnosis and missed diagnosis.

Materials and methods

Case selection. A total of 36 cases of lipoblastoma that were surgically resected and diagnosed at Shengjing Hospital of China Medical University, Shenyang, China, between January 2015 and January 2021 were collected. There were 22 males and 14 females, aged between 7 days and 33 years. Inclusion criteria included histopathologically confirmed lipoblastoma or lipoblastomatosis with hematoxylin- and eosin-stained sections, paraffin blocks and clinical data (age, sex, tumor location, size, surgery, complications and follow-up) available for all cases. Cases with missing IHC (S-100, CD-34, P-16 and desmin) analysis and cases with poorly preserved tissue blocks were excluded. The Institutional Review Committee of the hospital approved the study (ethical approval no. 2022PS104J). The need for written informed consent was waived in view of the retrospective nature. All cases were reviewed by two pediatric pathologists and lipoblastoma was classified into three subtypes: Classic, lipoma-like, and myxoid, as previously described (17,31).

Immunohistochemistry. All specimens were surgically excised, fixed in 3.7% neutral formaldehyde at room temperature for 24 h, routinely embedded in paraffin, sliced to 4-5 um thickness and stained with hematoxylin and eosin for ~45 min at room temperature by Roche fully automated system (VENTANA HE600; Roche) and histological characteristics were observed under a light microscope (DM 2500; Leica GmbH). The lesion area was selected and 3-μm-thick formalin-fixed paraffin-embedded sections were subjected to immunohistochemical staining with S-100, CD34 (cytoplasmic), desmin (cytoplasmic), and P16 using Envision kit (Elabscience Biotechnology Co., Ltd.) according to the manufacturer's instructions. Paraffin-embedded tissues were submerged three times in xylene for 5 min each. The sections were washed in 95% ethanol for 2 min, 90% ethanol for 2 min, 85% ethanol for 2 min, 80% ethanol for 2 min, 75% ethanol for 2 min and distilled water for 2 min to remove the xylene. The sections were then placed in EDTA PH 9.0 Antigen Repair Solution (E-IR-R104, Elabscience Biotechnology Co., Ltd.) for 20 min at 95 ˚C. After cooling to room temperature, the sections were removed. Place in distilled water for 5 min. Submerge sections in 3% H_2O_2 (E-IR-R115, Elabscience) for 10 min at room temperature. Rinse well with distilled water. Rinse 3 times with PBS buffer for 5 min each. Drop ready-to-use goat serum (E-IR-R217A, Elabscience) and block for 30 min at room temperature. Primary antibody was added at 4˚C for 12 h. Rinse 3 times with PBS buffer for 5 min each. Add ready-to-use polyperoxidase-anti-mouse/rabbit IgG (E-IR-R214B, Elabscience) at room temperature for 30 min. Rinse 3 times with PBS buffer for 5 min each. Add freshly prepared 20x diluted to 1x DAB developer (E-IR-R214D, Elabscience) for approximately 2-3 min. The sections were submerged in Mayer hematoxylin stain for approximately 5 min, washed with water to remove the stain, rapidly fractionated with 1% ethanol hydrochloride for 30 seconds, rinsed with tap water, and returned to blue for 1 min. Sections were sequentially placed in 75% ethanol for 1 min, 80% ethanol for 1 min, 90% ethanol for 1 min, 95% ethanol for 1 min, anhydrous ethanol twice for 3 min each, submerged in xylene twice for 5 min, and xylene (second) for 5 min, and the tissue was sealed by adding neutral gum dropwise on a coverslip. Primary antibodies were as follows: S-100 rabbit polyclonal (cat. no. ZA-0225, ready-to-use), CD34 rabbit monoclonal

(cat. no. ZM-0046, ready-to-use), P16 mouse monoclonal (cat. no. ZM-0205, ready-to-use) and desmin rabbit monoclonal (cat. no. ZA-0610, ready-to-use), purchased from Zhongshan Jinqiao Biotechnology Co., Ltd. Staining intensity and positive area were independently interpreted by two pathologists.

FISH. FISH detected the breakage and rearrangement of PLAG1 (8q12; gene ID: 5324). A PLAG1 mRNA probe (cat. no. CL-003; HealthCare Biotechnology Co., Ltd.) was designed and synthesized using cDNA as a template. The length of the probe was 1,090 kb. Total RNA was extracted from 50 mg lipoblastoma tissue stored at -80˚C using RNAiso Plus (cat. no. 9108; Takara Biotechnology Co., Ltd.) and RNase-free (cat. no. 2270A; Takara Biotechnology Co., Ltd.), followed by PrimeScript™ RT kit (dNTP and RNase Inhibitor are included) (cat. no. RR037A; Takara Biotechnology Co., Ltd) for RT using PLAG1 forward primer: GCCGCAACA AGTGGTGACCTC; reverse primer: CCAGACGACTTGCCT GCATGAG. Thermocycling: pre-denaturation 95˚C, 5 min; 95˚C, 15 sec, PCR reaction 60˚C for 1 min, 35 cycles; solubility curve phase 95˚C, 15 sec, 50˚C, 1 min, 95˚C, 30 sec. The target gene cDNA fragment was inserted into a plasmid (cat. no. 3340; Takara Biotechnology Co., Ltd.) containing a specific RNA polymerase (cat. no. 2520A; Takara Biotechnology Co., Ltd.) promoter sequence, and the recombinant plasmid was then amplified, purified. The plasmid template was cleaved with restriction enzyme (cat. no. 1060A/B; Takara Biotechnology Co., Ltd.) to linearize. And then under the action of RNAase (cat. no. RR420Q; Takara Biotechnology Co., Ltd.), starting from the promoter site, the cDNA was used as a template for *in vitro* transcription. In the *in vitro* transcription reaction system, nucleotide feedstock with digoxigenin labeling is provided, and the labeled RNA probe is obtained after *in vitro* transcription. The nucleotide sequences were PLAG1-red end: CTD-2245E20, CTD-2124P3, CTD-2359C13; PLAG1-green end: CTD-2283H1, RP11-22I14, CTD-2005O24, CTD-2344J3, CTD-2266F8, CTD-2130C19. Paraffin tissue sections of 3 μm thickness were selected and baked at 65˚C for 2 h. Sections were dewaxed: xylene 10 min x2 times, 100, 85, 70% gradient ethanol rehydration (5 min/cylinder), deionized water rinsing. Sections were placed in distilled water at 100˚C for 25 min, covered with pepsin (20 μg/ml; cat. no. 9001-75-6; Guangzhou LBP Medicine Science and Technology Co., Ltd.), incubated at 37˚C for 20 min, and then incubated with 2x saline-sodium citrate (SSC; cat. no. 6132-04-3; Guangzhou LBP Medicine Science and Technology Co., Ltd.) for 10 min x2 times at room temperature, fixed in ethanol gradient dehydration and dried. Using a ThermoBrite *in situ* hybridizer (S500-24; Leica), the probe was co-denatured with the tissue in hybridization buffer at 85˚C for 5 min and hybridized at 42˚C for 16 h. Gradient washes were performed under SSC buffer (2X SSC at 37˚C for 1 min, 1X SSC at 37˚C for 10 min, 0.5X SSC at 37˚C for 10 min). The slides were placed in pre-warmed 0.3% NP-40/0.4X SSC at 68˚C for 2 min. The sections were removed and immersed in pre-warmed deionized water at 37˚C for 1 min. The slides were dried naturally in the dark. No blocking reagent was applied in this experiment. DAPI re-staining agent (5 μg/ml; cat. no. 220401; HealthCare Biotechnology Co., Ltd.) was dropped onto the hybridized area, immediately covered with a coverslip, and then observed under a fluorescence microscope at 100x magnification (Axio Imager.A2; ZEISS). PLAG1 breaks were considered positive if ≥10% of at least 100 cells (positive control, salivary gland tumors from HealthCare Biotechnology Co., Ltd.) showed PLAG1 breaks. The results were analyzed using Isis software version 5.9.1 (MetaSystems).

Statistical analysis. SPSS 26.0 software (IBM Corp.) was used for statistical analysis of clinical pathological data. Values are expressed as median. Continuous variables that conformed to normal distribution were analyzed by one-way ANOVA with LSD method for post hoc tests and continuous variables that did not conform to normal distribution were analyzed by Kruskal-Wallis rank sum test. Fisher's exact test was used for categorical variables. $P<0.05$ was considered to indicate a statistically significant difference. Disease-free survival curves were constructed using the Kaplan-Meier method.

Results

Clinical features. Clinicopathological characteristics of lipoblastoma series (n=36) are shown in Tables I and II. The study included 22 males and 14 females (male to female ratio, 1.6:1.0) with age ranging from 7 days to 33 years (median, 1.5 years; mean, 3.2 years). A total of 28 and eight patients were aged ≤3 and >3 years (8/36, 22%), respectively. The median ages of patients with classic, lipoma-like and myxoid subtypes were 10 months (range, 7 days to 3 years), 2 years (range, 10 months to 7 years) and 4 years (range, 3 months to 33 years), respectively. There was a significant difference in age between the groups. The sites included the extremities (n=12, 33%), head and neck (n=6, 17%), trunk (n=16, 44%) and perineum (n=2, 6%); in most cases, the site was the abdomen (8/36 cases, 22%). Tumor size ranged from 1.7 to 16.2 cm (median, 4.7 cm; mean, 5.5 cm), without statistically significant differences between subtypes. In our case, lipoblastoma was more frequent in males, in patients no older than 3 years of age, and in the extremities. Patients are slightly older in the mucinous subtype.

Myxoid lipoblastomas were yellow-to-white, medium in texture and partly translucent. Classic and lipomatous lipoblastomas appeared more homogeneous, with a yellow appearance and medium texture, accompanied by fibrous septa and localized hemorrhage. Histologically, all subtypes of lipoblastoma exhibited fibrous septa (data not shown). Classic lipoblastoma (n=15) had lobular architecture and variable amounts of mature adipose tissue, with scattered lipoblasts, spindle cells and myxoid stroma accounting for <50% of the section (Fig. 1A). This subtype presented with mature banded morphology and a small amount of plexiform vascular tissue with a predominantly myxoid background. The lipoma-like subtype (n=13) consisted primarily of mature adipocytes of varying sizes surrounded by fibrous tissue with few lipoblasts or myxoid stroma (Fig. 1B). Myxoid lipoblastomas (n=8) were cytologically diverse, with a myxoid background accounting for >50% of the entire morphology, including a myxoid pool, stellate- and spindle-shaped primitive mesenchymal cells, a small number of adipocyte components, no pathological mitosis (Fig. 1C) and vascular plexiform, resembling myxoid liposarcoma.

Molecular characteristics. FISH identified *PLAG1* breakage and rearrangement in 24 of 32 (75%) lipoblastoma

Table I. Characteristics of 36 patients with lipoblastoma.

Characteristic	Total (n=36)	Classic subtype (n=15)	Lipoma-like subtype (n=13)	Myxoid subtype (n=8)	P-value
Male	22	9	8	5	1.00[a]
Age, months					0.01[b]
Mean	38.98	15.08	33.08	93.38	
Median (range)	18.00 (0.23-396)	10 (0.23-36)	24 (10-84)	48 (3-396)	
Location					0.91[a]
Extremities	12	4	5	3	
Head and neck	6	4	1	1	
Trunk	16	6	6	4	
Perineum	2	1	1	0	
Size, cm					0.24[c]
Mean	5.54	4.58	6.46	5.85	
Median (range)	4.70 (1.70-16.20)	4.00(2.50-8.20)	5.60 (1.70-16.20)	5.10 (2.20-10.50)	
S-100+	29	12	10	7	1.00[a]
CD-34+	36	15	13	8	-
P-16+	8	5	0	3	0.03[a]
Desmin+	26	9	10	7	0.40[a]
FISH *PLAG1*+	24	11	8	5	1.00[a]

[a]Fisher's exact test; [b]Kruskal-Wallis rank sum test; [c]one-way ANOVA. -, not applicable; FISH, fluorescence *in situ* hybridization; *PLAG1*, pleiomorphic adenoma gene 1.

samples (Table II). There were no statistically significant differences between the subgroups (Table I). Representative FISH images are shown in Figs. 2 and 3. The *PLAG1* gene breakage probe uses orange-red dye to label *PLAG1* 3' end region (460 kb) and green dye to label the *PLAG1* 5' end region (580 kb) with the 50 kb PLAG1 gene in the middle. In Fig. 2, orange-red and green signal are separated in the tumor cells, which represents breakage and rearrangement of *PLAG1* in this tumor cell. By contrast, in Fig. 3, tumor cells did not undergo breakage and rearrangement of *PLAG1* so the orange-red and green signals were not separated. In the classic and myxoid subgroups of lipoblastoma, FISH-negative detection rates were 27 and 29%, respectively, compared with 20% in the lipoma-like subtype. Therefore, the highest probability of *PLAG1*-positive rearrangement was detected using FISH in the lipoma-like subgroup. Also, two of three relapsed patients tested negative for *PLAG1* fragmentation and rearrangement. One patient failed the trial. Although S-100, CD-34, P-16 and desmin IHC were not associated with recurrence in patients with lipoblastoma patients by Kaplan-Meier analysis (Fig. S1A-D), patients with positive PLAG1 fragmentation and rearrangement had a risk of relapse of only 0.57% of those with negative PLAG1. Patients who were positive for PLAG1 fragmentation and rearrangement had a 99.49% lower risk of recurrence than those who were negative (Fig. S1E). However, there were only 3 patients with recurrence in the present study, including one patient who was not detected, which requires further verification with large samples.

Immunohistochemical characteristics. Immunohistochemical results are presented in Table SI. S-100-positive mono- or multivesicular lipoblasts were observed (29/36, 81%), with occasional mature adipocytes (Fig. 1F). CD34 (36/36, 100%) staining was diffusely strong in the cytoplasm of primitive spindle mesenchyme and peripheral vessels and abundant in blood vessels, highlighting a zonal pattern (Fig. 1G). Most tumor cells were negative while only few were positive for P16 (8/36, 22%; Fig. 1H). Desmin (26/36, 72%) staining was positive in primitive mesenchymal cells and striated muscle tissue in the dense fibrous septum (Fig. 1I). However, P16 IHC was less likely to be expressed in the lipoma-like subtype than in the other two subtypes (Table I).

Follow-up. In total, 28 cases were clinically followed up (range, 2-84 months; median, 41 months), of which 3 patients relapsed, 8 were lost to follow-up and others were alive without disease.

Discussion

Here, 36 lipoblastoma cases underwent morphological, S-100, CD34, desmin and P16 immunohistochemical and *PLAG1* FISH analysis. Other studies with similar sample size have mainly focused on the morphology and immunophenotyping (19,32). However, the present study attempted to diagnose at the molecular level. Similar to other cases (17-20), the majority of the present cases (28/36, 78%) were detected within three years of age. By contrast with the large series studied by Coffin *et al* (19) (n=59), who reported a range of clinical associations in up to 17% of lipoblastomas, the present study did not identify any syndromic association, except for one case with complications of subcutaneous emphysema (case 20). According to other reports, more than one-fifth of

Table II. Clinicopathological characteristics of lipoblastoma.

A, Classic subtype (n=15)

Case	Sex/age	Location	Size, cm	*PLAG1* FISH	Complete resection	Follow-up, months
2	M/7 m	Left armpit	5.6x5.4	+, 69%	Yes	AWOD, 78
3	M/10 m	Retroperitoneum	4.8x4.8	+, 30%	Yes	Lost to follow-up
4	F/6 m	Right neck	2.8x2.2	+, 39%	Yes	AWOD, 74
8	F/7 m	Right armpit	8.0x5.0	+, 28%	Yes	Lost to follow-up
10	M/1 y	Neck	4.0x3.0	-, 2%	Yes	AWOD, 64
12[a]	F/7 d	Abdominal wall	4.2x3.5	-, 2%	Yes	Lost to follow-up
15	M/3 y	Left scapular region	8.2x5.2	+, 35%	Yes	Lost to follow-up
16[a]	M/10 m	Armpit	3.1x3.1	+, 33%	Yes	AWOD, 54
18	F/1 y	Supraclavicular fossa	2.5x2.0	-, 6%	Yes	AWOD, 53
19	M/8 m	Left maxilla	3.0x2.0	-, 3%	Yes	AWOD, 54
20	M/10 m	Mediastinum	4.0x4.0	+, 39%	Yes	Lost to follow-up
22	M/1 y	Perineum	3.8x2.7	+, 35%	Yes	AWOD, 39
25	M/2 y	Left armpit	5.7x5.0	+, 32%	Yes	AWOD, 31
31	F/3 y	Left chest wall	2.8x2.2	+, 57%	Yes	AWOD, 11
32	F/3 y	Right upper mediastinum	6.2x5.2	+, 45%	No	AWOD, 5

B, Lipoma-like subtype (n=13)

Case	Sex/age	Location	Size, cm	*PLAG1* FISH	Complete resection	Follow-up, months
7[a]	M/2 y	Left chest wall	6.0x4.0	-, 1%	No	AWOD, 68
11	M/2 y	Scrotum	1.7x1.3	+, 22%	Yes	AWOD, 63
13	M/5 y	Abdominal cavity	5.6x4.6	+, 35%	Yes	AWOD, 57
14[a]	F/3 y	Right parotid gland	3.4x3.3	ND	Yes	AWOD, 57
17	M/3 y	Right upper arm	7.2x5.0	-, 5%	Yes	Relapse after 54 months
21	F/1 y	Right popliteal fossa	9.7x5.0	+, 42%	Yes	AWOD, 43
23[b]	M/5 y	Mesentery	3.0x3.0	ND	NO	Relapse after 51 months
26	M/3 y	Mesentery	16.2x13.8	+, 31%	Yes	AWOD, 29
27	M/1 y	Right thigh	5.4x3.3	+, 23%	Yes	AWOD, 26
29	F/10 m	Abdomen	7.7x6.5	ND	Yes	AWOD, 18
30	F/7 y	Right foot	4.5x2.2	+, 42%	Yes	AWOD, 16
34	M/2 y	Left hip	4.1x2.6	+, 26%	Yes	AWOD, 3
35	F/1 y	Mesentery	9.5x9.4	+, 45%	Yes	AWOD, 3

C, Myxoid subtype (n=9)

Case	Sex/age	Location	Size, cm	*PLAG1* FISH	Complete resection	Follow-up, months
1	M/4 y	Right shoulder	4.6x4.4	+, 32%	Yes	Lost to follow-up
5[a]	F/3 m	Behind the right ankle	2.2x1.8	+, 41%	Yes	Lost to follow-up
6[a]	M/11 y	Right sole	3.8x2.8	+, 50%	Yes	AWOD, 71
9	M/8 y	Left thigh	10.0x5.0	-, 2%	Yes	Lost to follow-up
24[a]	M/1 y	Back	7.1x2.3	ND	Yes	AWOD, 32
28	M/33 y	Mediastinum	10.5x3.5	-, 2%	No	Relapse after 15 months
33	F/4 y	Right thoracic cavity	5.6x3.4	+, 82%	Yes	AWOD, 3
36	F/1 y	Neck	3.0x2.9	+, 47%	Yes	AWOD, 2

[a]Case was lipoblastomatosis, infiltrating the skeletal muscle tissue; [b]primary tumor was 15x12x11 cm at the age of 1 year and recurred 51 months after incomplete resection, but the patient survived without disease for 33 months after re-excision. F, female; M, male; d, days; m, months; y, years; FISH, fluorescence *in situ* hybridization; AWOD, alive without disease; ND, not detected; *PLAG1*, pleiomorphic adenoma gene 1.

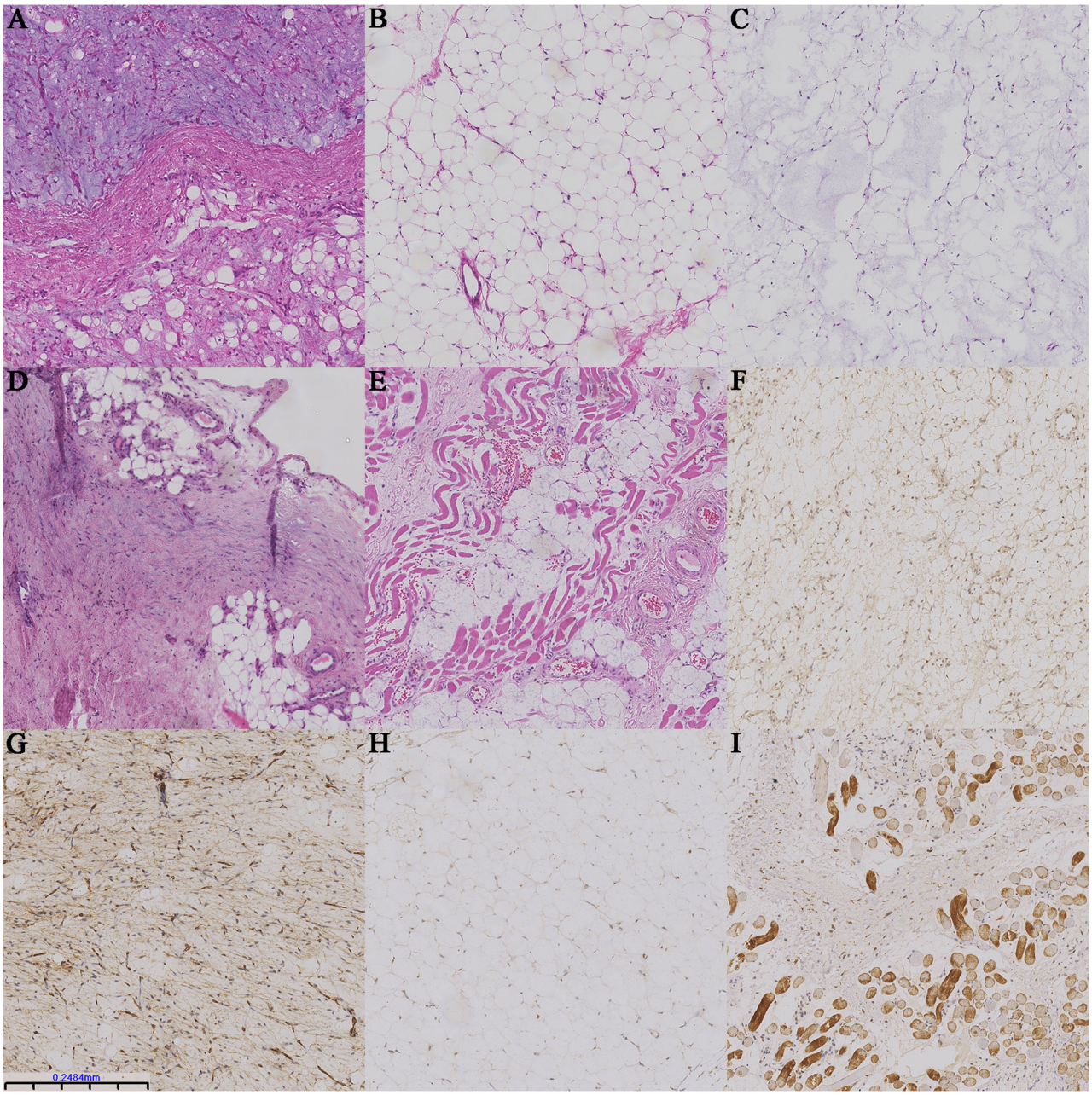

Figure 1. Histopathology classification and immunohistochemical expression of lipoblastoma and lipoblastomatosis. (A) Classical lipoblastoma. Background is myxoid, with lobular structure and varying amounts of mature adipose tissue. (B) Lipoma-like lipoblastoma. Mature adipocytes of varying size, surrounded by fibrous tissue. (C) Myxoid lipoblastoma with a myxoid background accounting for >50% of the entire morphology, with obvious mucin pools. (D) Fibroblast lipoblastoma showing obvious fibrous stroma, mild spindle cells without atypia. (E) Lipoblastomatosis. Tumor cells infiltrating the skeletal muscle tissue. (F) Single or multivesicular lipoblasts positive for S-100. (G) Primitive mesenchymal cells and peripheral blood vessels diffusely strongly positive for CD34. (H) No expression of P16 in a case of lipoblastoma. (I) Rhabdoid muscle tissue and primitive mesenchymal cells in fibrous cell bundles strongly positive for desmin in a case of lipoblastoma.

lipoblastomas occur in patients >3 years of age, consistent with the proportion reported in the present study (17,31). The present findings differ from those of other studies showing that lipoblastoma occurs most frequently in extremities, since lipoblastomas in the present cases occurred most frequently in the trunk (19,32-35). The patients were predominantly male and exhibited median tumor size of 4.7 cm. In certain studies, the recurrence rate in children reached 25% (1,6); here, only 3 (8%) recurrences occurred, 2 of which recurred because the tumor was too close to the adjacent organ with incomplete resection (in case 23, following recurrence the patient returned for further resection and was diagnosed with lipoma-like lipoblastoma, which matured into lipoma). The reason may be that the infant had relapsed after 51 months and the lipoblasts had matured and progressed. In another case (case 17), recurrence occurred *in situ* in the superficial subcutaneous fascia of the right upper arm 54 months after complete resection. The longest (case 17) and shortest (case 28) intervals between recurrences were 54 and 15 months, respectively.

Notably, recurrence occurred in two of four patients (50%; at 1 and 33 years of age, respectively) with incomplete tumor resection; three patients (case 7, 23, and 32) were young and

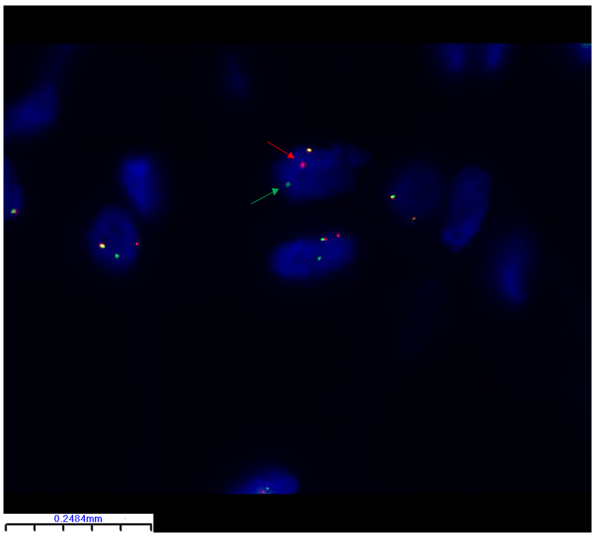

Figure 2. *PLAG1* breakage and rearrangement detected with fluorescence *in situ* hybridization using two-color separation probe in lipoblastoma (case 25). The *PLAG1* gene breakage probe uses orange-red dye to label *PLAG1* 3' end region (orange arrow) and green dye to label the *PLAG1* 5' end region (green arrow) and detects *PLAG1* breakage and rearrangements. *PLAG1*, pleiomorphic adenoma gene 1.

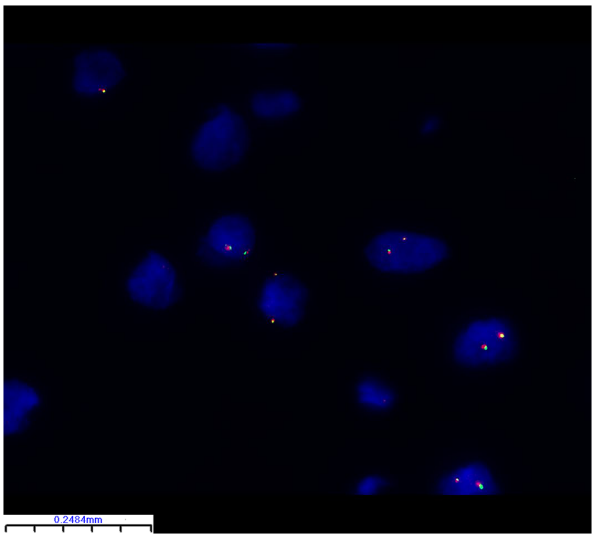

Figure 3. Fluorescence *in situ* hybridization did not detect *PLAG1* breakage and rearrangements using two-color separation probe (case 19). The region of the *PLAG1* gene between the orange-red and green staining is not disrupted. *PLAG1*, pleiomorphic adenoma gene 1.

one (case 28) was older. It was hypothesized that patients with incompletely resected tumors are more likely to relapse regardless of age.

The clinical outcome primarily depends on the completeness of resection, with a high recurrence rate in incompletely resected tumors. Close follow-up for at least five years is recommended (6). A total of seven cases had lipoblastomatosis characterized by a diffuse growth pattern, including two classic and lipoma-like subtypes and three myxoid subtypes; these histological characteristics are similar to those of lipoblastomas (34). Similar to intramuscular lipoma, residual skeletal muscle tissue can be observed in lipoblastomatosis, but without recurrence (5). Dao *et al* (36) conducted a meta-analysis and found that lipoblastomatosis has a higher risk of recurrence than localized lipoblastoma (odds ratio=5.1; 95% confidence interval, 1.9-15.9).

The primary genetic feature of lipoblastoma is chromosomal translocation (minor inversions, insertion and circular chromosomes), resulting in the rearrangement of *PLAG1*, which encodes a zinc finger transcription factor that is expressed during fetal life and is present at low levels or absent in most adult organs (9). In lipoblastoma, exons 2 or 3 of *PLAG1* most commonly combine with exon 1 at the N-terminus of partner genes (the fourth exon is the coding region containing the initiation codon) (12) so that the entire coding sequence is retained under transcriptional control of a more active promoter (37), resulting in subsequent upregulation (14,38). In a mouse model, overexpression of *PLAG1* was found to induce tumorigenesis (39). Here, 75% of cases showed *PLAG1* breakage and rearrangement, greater than the 60-70% reported in the literature (31,34,38). Coiled-Coil-Helix-Coiled-Coil-Helix Domain Containing 7 (*CHCHD7*)-*PLAG1* fusion, which also results in promoter swap and *PLAG1* activation, has been reported as a recurrent event in salivary gland pleomorphic adenoma (40-42). Two studies reported that hyaluronan synthase 2 (*HAS2*) (8q24.1) and serine and arginine rich splicing factor 3 (*SRSF3*) (6p21.3-p21.1) fusion genes are prone to local recurrence in lipoblastoma (9,28). At present, RNA next-generation sequencing (NGS) serves a key role in the classification and diagnosis of soft tissue tumors, including defining the tumors, especially in cases where the morphology is atypical and immunohistochemistry cannot indicate the specific tumor type (31). It has been suggested that even if FISH and immunohistochemistry results are negative, the tumor may still be a lipoblastoma because high mobility group at-hook 2 (*HMGA2*) is an upstream regulatory activator of *PLAG1* (43). In the absence of chromosome 8 abnormality involving the *PLAG1* locus, *HMGA2* induces activation and overexpression of *PLAG1*; therefore, *PLAG1* FISH and immunohistochemistry results may be negative in cases with *HMGA2* rearrangement.

PLAG1 expression has been observed in the absence of *PLAG1* rearrangements, suggesting an alternative mechanism underlying alterations in genes upregulates *PLAG1* expression, such as increasing the *PLAG1* copy number, as proposed previously (38,44). Thus, the diagnostic role of *PLAG1* immunohistochemistry is limited, particularly in morphologically difficult cases of mature lipoblastoma, where only sparsely positive immature adipocytes and spindle cells are typically identified; this finding is consistent with the results of Lopez-Nunez *et al* (17). However, if *PLAG1* FISH is positive in adipose tumor, an accurate diagnosis can be made using a combination of morphology and immunohistochemistry. Therefore, it was hypothesized that when lipoblastoma is suspected, FISH detection of *PLAG1* may replace *PLAG1* immunohistochemistry.

Moreover, NGS not only detects *PLAG1* or *HMGA2* rearrangements with high sensitivity but also identifies *PLAG1*-associated fusion genes. Numerous fusion gene partners [dead-box helicase 6 (*DDX6*), klf transcription factor 10 (*KLF10*), kat8 regulatory nsl complex subunit 1 like (*KANSL1L*), hyaluronan synthase 2 (*HAS2*), collagen type III alpha 1 chain (*COL3A1*), rad51 paralog b (*RAD51L1*), collagen type I alpha

2 chain, ras-related protein rab-2a (*RAB2A*), *CHCHD7*, serine and arginine rich splicing factor 3 (*SRSF3*), heterogeneous nuclear ribonucleoprotein c (*HNRNPC*), protein-l-isoaspartate (d-aspartate) o-methyltransferase domain containing 1 (*PCMTD1*), tyrosine 3-monooxygenase/tryptophan 5-monooxygenase activation protein zeta (*YWHAZ*), ctd small phosphatase 2 (*CTDSP2*), protein phosphatase 2 regulatory subunit α, boc cell adhesion associated, oncogene regulated, zinc finger e-box binding homeobox 2, runx1 partner transcriptional co-repressor 1, Versican, peptidase inhibitor 15 and eukaryotic translation elongation factor 1 alpha 1] with *PLAG1* have been identified in lipoblastoma (8,14,17,31,37,44-52). These fusions lead to overexpression of *PLAG1* (17,37). Although only the *YWHAZ* promoter is fused to *PLAG1*, it does not contribute to protein expression (49). The rearrangement of *PLAG1* [a transcriptional activator of Insulin Like Growth Factor 2 *(IGF2)*] in lipoblastoma activates the *MAPK* and *PI3K/AKT* signaling pathways by directly increasing expression of *IGF2* and promoting the differentiation of CD34-positive primitive mesenchymal cells into lipoblasts (14,53). Pleomorphic adenoma and lipoblastoma with *PLAG1* rearrangement differ in their partner genes (13,54). In salivary gland tumors, the primary targets of translocation are DNA-binding transcription factors (*PLAG1* and *HMGA2*) involved in growth factor signaling and cell cycle regulation as well as co-activators of Notch [mastermind like transcriptional coactivator 2, (*MAML2*)] and cAMP [target of rapamycin complex 1, (*TORC1*)] signaling pathways. These fusion genes, which are also involved in molecular tumor pathways, serve a key role in tumorigenesis. Therefore, timely identification of the associated genetic alterations and molecular classification of these childhood lesions are important for proper follow-up, evaluation of potential recurrence and avoidance of secondary surgery.

The histological diagnosis of lipoblastoma with typical morphological features is relatively straightforward in infancy and early childhood. In first-born infants, tumors are predominantly composed of primitive mesenchymal cells with extensive myxoid stromal and minimal lipoblastoid components; therefore, primitive myxoid mesenchymal tumor of infancy (PMMTI) should be considered, which exhibits a more aggressive behavior (55). PMMTI has typical cellular atypia, strong mitotic activity and distinct round cellular component compared with lipoblastoma, as reported by Warren *et al* (50). PMMTI can overlap with undifferentiated myxoid lipoblastoma, which resembles myxoid lipoblastoma. Notably, RNA NGS has been used to assess internal tandem repeats of BCL6 corepressor, a characteristic change in PMMTI (56). Lipoblastoma-like tumors of the vulva (LLTV) occur in adults, mostly commonly at age 17-46 years. Most often, LLTV presents as a unilateral, severely myxoid, gelatinous, well-circumscribed, lobulated vulvar mass. The morphology includes lobulated and varied proportions of mature adipocytes; mild lipoblasts; spindle cells with short, thick nuclei and prominent branching vessels with minimal nuclear atypia in a diffuse myxoid background. In LLTV, mitosis without necrosis is rare. Therefore, it also shows histological overlap with lipoblastoma (57). Here, two cases of lipoblastoma occurred in the perineal region (cases 11 and 22); both were males aged <2 years. FISH showed *PLAG1* rearrangement; therefore, LLTV was excluded. In children, the morphological appearance of a lipoma-like subtype requires differential diagnoses, including lipoma, lipofibromatosis, fibrous hamartoma of infancy, atypical lipomatous tumor/well-differentiated liposarcoma and non-neoplastic lesions with post-traumatic fat necrosis (such as post-traumatic pseudolipoma) (Table III). Microscopically, lipofibromatosis may have a spindle cell component in fascicular cells, lack lipoblasts and show more invasive growth in the surrounding tissue (58). In cases of post-traumatic fat necrosis, morphology is characterized by chronic inflammatory changes, fat necrosis and hematoma formation. A clinical history is helpful for diagnosis (59). Although lipoblastoma can be differentiated from liposarcoma based primarily on age, when lipoblasts mature, especially in older adults or deep in the limbs, mediastinum, abdominal pelvis or retroperitoneum, they tend to be larger. In these cases, tumors present with extensive myxoid or lipomatous morphology and rare lipoblasts, especially focal adipocytes and stromal cells, with nuclear atypia and local invasiveness. In such cases, other diseases such as myxoid liposarcoma and atypical lipomatous tumor/well-differentiated liposarcoma should be considered (58,60). With fine-needle biopsy specimens, it is difficult to histologically distinguish lipoblastoma, which may require further molecular detection (61). (*PLAG1* and *DDIT3*) and (*PLAG1* and *MDM2*) genetic fusion testing may confirm this diagnosis. In addition, insulin-induced lipoatrophy should be considered if there is a clinical history of diabetes or malnutrition, as these cases may exhibit myxoid changes and pseudolipoblasts (62). The morphology of the classic subtype of lipoblastoma is more typical (31). In case 34, lipoblastoma with fibroblast morphology which is the fourth class of lipoblastoma (31) was focally present but surrounded by classic lipoblastoma. Thus, it was classified as a classic subtype. The fifth class of lipoblastoma, consisting primarily of multivacuolar lipoblasts, some of which have central nucleus and granular eosinophilic cytoplasm lacking a myxoid component, was not observed in the present study. The tumor was named lipoblastoma with hibernoma-like features (38). Studies have reported that P16 effectively differentiates benign lesions from liposarcoma (24,63). It is necessary to combine CD34-positive primitive mesenchymal cells with a more characteristic histological morphology in lipoblastoma with clinical information and biological behavior to diagnose lipoblastoma. Clinical features, histological morphology, biological behavior, immunohistochemical expression, and genetic changes of the 12 tumors that are difficult to differentiate from lipoblastoma are summarized in Table III.

In clinical practice, rapid FISH detection is favored by pathologists for soft tissue tumors because of its rapidity, low cost and high diagnostic efficiency. Here, the frequency of *PLAG1* rearrangement (75%) in lipoblastoma was higher than that reported in previous studies (17,38); however, 4 lipoblastomas were not successfully detected. Quality control review was performed to rule out factors that were more likely to be associated with short formalin fixation time, too old specimens and DNA degradation. In addition, the present study lacked a control group for other adipose tumors and only tested *PLAG1* for lipoblastoma.

In the classic and myxoid subgroups of lipoblastoma, FISH-negative detection rates were 27 and 29%, respectively,

Table III. Clinicopathological features of the differential diagnoses of lipoblastoma.

A, Lipoblastoma with predominant myxoid morphology

Diagnosis	Features	First author, year (Refs.)
Myxoid liposarcoma	Myxoid liposarcoma is rare in children, usually occurs in 30-60-year-old adults. Histomorphologically, mature adipocytes in the lobules are concentrated in the periphery, whereas in lipoblastoma, maturation occurs in the center of the lobule and the periphery is composed of more primitive cells, lacking the enrichment phenomenon cells around blood vessels. The focal nuclei are atypic and pleomorphic, with pathological mitosis. A characteristic pulmonary edema morphology is observed due to the pooling of matrix mucins. Tumor cells express S-100 protein and NY-ESO-1 to varying degrees and are negative for CD34, desmin, keratin, SMA, MDM2 and CDK4. In this tumor, rearrangement of chromosome 12q13 (CHOP/DDIT3) with translocation partners 16p11 (FUS-TLS) or 22p11 (EWSR1) results in disruption of the CHOP gene on chromosome 12.	Coffin, 2012 (58)
PMMTI	PMMTI primarily occurs in infants, mainly on the trunk, neck, and extremities. Histomorphologically, there are mainly round cell components, primitive mesenchymal cells and myxoid matrix, curvilinear-plexiform vascular morphology, pseudolipoblasts, cellular atypia, and frequent mitosis. S-100 expression is negative on histochemistry. BCOR-ITD or YWHAE gene rearrangement and lack of PLAG1 gene rearrangement are seen in this tumor.	Warren, 2021 (47); Deen, 2013 (52); Andersson, 2019 (53)
Invasive angiomyxoma	Invasive angiomyxoma primarily occurs in young and middle-aged females. Histomorphologically, there are spindle and asteroid cell with unclear boundaries, thin-walled or thick-walled blood vessels of varying sizes distributed in a myxoid matrix rich in slender collagen fibers, atypical tumor cells, small round or oval nuclear, and no mitosis. Tumor cells express vimentin, desmin, ER, and PR; most nuclei express HMGA2; CD34 and S-100 are not expressed. HMGA2 (12q14.3) rearrangement is seen in this tumor.	Yang, 2021 (28)
LLTV	LLTV primarily occurs in adult females, primarily in the vulva or groin. Histomorphologically, there are lobular appearance, mature adipocytes interspersed with spindle cells, lipoblasts, myxoid matrix, branching vessels, and no banded mature morphology. On histochemistry the tumor loses nuclear expression of RB protein (usually mosaic morphology) and is negative for S-100, PLAG1, and HMGA2 expression. The tumor has no DDIT3T fusion and no evidence of PLAG1 gene alteration, and associates with chromosomal 13q alteration.	Stenman, 2005 (54)
Lipoatrophy	Lipoatrophy primarily occurs in adults with a clinical history of insulin-dependent diabetes or starvation (malnutrition or anorexia). Histomorphologically, there are presence of lobular architecture, myxoid changes, and pseudolipoblasts.	Jermendy, 2000 (62)
Superficial angiomyxoma	Superficial angiomyxoma is rare in infants and young children, more common in middle-aged people (median age 40 years). Histomorphologically, there are abundant myxoid matrix, sparse spindle or asteroid cells, and slender capillaries, lobulated structures with indistinct boundaries. Lack of lipoblasts at different developmental stages are key to differential diagnosis. Tumor cells express CD34; some cells are positive for SMA, MSA, and desmin; S-100 is not expressed.	Iwashita, 2020 (29)

B, Lipoblastoma with predominant mature lipoma-like morphology

Diagnosis	Features	First author, year (Refs.)
Lipofibromatosis	Lipofibromatosis primarily occurs in infants (congenital subgroup) to 14 years of age. Histomorphologically, there are infiltration in skeletal muscle, spindle cell components forming long thin fascicles, mature adipose tissue, and absent of lipoblasts. Spindle cells express vimentin, CD34, and	Mirkovic, 2015 (57)

Table III. Continued.

B, Lipoblastoma with predominant mature lipoma-like morphology

Diagnosis	Features	First author, year (Refs.)
	a-SMA to varying degrees and can express S-100 focally, but not desmin. Activation of EGFR (HER1), EGFR, ROS1, RET, or PDGFRB may indicate pathogenesis.	
ALT/WDLPS	ALT/WDLPS primarily occurs in middle-aged and elderly; peak age of onset is 50-60 years. Histomorphologically, there are focally seen nuclear heterogeneity or hyperchromasia. Neoplastic adipocytes and atypical stromal cells express MDM2, CDK4, and P16. MDM2 gene amplification is the gold standard for identifying benign fatty tumors and ALT/WDLPS.	Alaggio, 2009 (60)
Post-traumatic pseudolipoma	Post-traumatic pseudolipoma can occurs in all age groups. Histomorphologically, there are foam cells, adipocytes surrounding necrotic tissue, showing pseudoadenoid structures, multinucleated giant cells with hyperchromatic nuclei, and interstitial inflammatory cells. Adipocytes express S-100, histiocytes express CD68. Diagnosis of the disease requires a combination of medical history and gross structure.	Aust, 2007 (59)
Lipoma	Lipoma primarily occurs in adults. Histomorphologically, there are rarely seen lobulated structures, lipoblasts, and areas of mucinous stroma with plexiform capillaries. Lipomas can be misdiagnosed when they are associated with extensive myxoid degeneration. Tumor cells express S-100 and HMGA2; no express MDM2 and CDK4.	Abdul-Ghafar, 2018 (25)
Fibrous hamartoma of infancy	Fibrous hamartoma of infancy primarily occurs in infants, is usually less than 2 years old, and is more common in boys. Histomorphologically, there are characteristic organ growth structures, including bland fibroblasts/myofibroblasts, primitive mesenchymal cells, and mature adipose tissue, without lipoblasts/pseudolipoblasts. CD34 is only diffusely expressed in collagenized pseudoangioma-like (or neurofibromatous) areas; mature adipose tissue express S-100. EGF expression is rarely detected. EGFR exon 20 insertion/repeat mutation are seen in this tumor.	Al-Ibraheemi, 2017 (30)
Hibernoma	Hibernoma primarily occurs in young and middle-aged people (20-40 years old). Brown adipocyte component is more prominent, with a central nucleus and abundant fine-grained eosinophilic cytoplasm. Tumor cells express S100 in varying degrees, and the spindle cell subtype express CD34.	Gisselsson, 2001 (38)

PMMTI, primitive myxoid mesenchymal tumor of infancy; ALT/WDLPS, atypical lipomatous tumor/well-differentiated liposarcoma; LLTV, lipoblastoma-like tumor of the vulva.

compared with 20% in the lipoma-like subtype. The higher negative detection rate in the first two groups indicated that in certain cases, lipoblastoma may not result in cytogenetic segregation of the target gene, which leads to undetected rearrangements by FISH (64). RNA NGS may improve diagnostic accuracy. Therefore, RNA NGS is necessary, especially for uncommon age groups or morphologically atypical populations. Lipoblastomas mature into regular lipomas or are similar to fibrolipoma (25,34). Here, subjects with a median age of up to three years had the lipoma-like subtype. Whether older individuals have a higher tendency to develop the lipoma-like subtype or mature lipoma requires further experimental verification, clinical observation and molecular characterization to clarify the occurrence and development of the disease.

Patients with lipoblastoma are usually within the age of three years; however, the disease cannot be ruled out in patients older than three years and may also occur in adults with mature adipose tissue with prominent lobular structures. Immunochemistry showing S-100-positive single or multivesicular adipocytes and CD34- and desmin-positive primitive mesenchymal cells as well as FISH results indicating *PLAG1* gene breakage and rearrangement are key to diagnosis and differential diagnosis.

Acknowledgements

Not applicable.

Funding

The present study was supported by the National Natural Science Foundation of China (grant no. 81601692), the

Technology Research from the Department of Education of Liaoning Province (grant no. JCZR2020013) and 345 Talent Project of Shengjing Hospital of China Medical University (grant no. M0367).

Availability of data and materials

All data generated or analyzed during this study are included in this published article.

Authors' contributions

WZ collected and analyzed data and wrote the paper. WZ, SZ, ZY and YZ performed immunohistochemistry and FISH. ZW conceived and supervised the study. WZ and ZW confirm the authenticity of all the raw data. All authors have read and approved the final manuscript.

Ethics approval and consent to participate

The study was approved by the Institutional Review Committee of Shengjing Hospital of China Medical University (approval no. 2022PS104J). The requirement for written informed consent was waived due to the retrospective nature of the study.

Patient consent for publication

Not applicable.

Competing interests

The authors declare that they have no competing interests.

References

1. Speer AL, Schofield DE, Wang KS, Shin CE, Stein JE, Shaul DB, Mahour GH and Ford HR: Contemporary management of lipoblastoma. J Pediatr Surg 43: 1295-1300, 2008.
2. Putra J and Al-Ibraheemi A: Adipocytic tumors in children: A contemporary review. Semin Diagn Pathol 36: 95-104, 2019.
3. Spătaru RI, Cîrstoveanu C, Iozsa DA, Enculescu A, Tomescu LF and Şerban D: Lipoblastoma: Diagnosis and surgical considerations. Exp Ther Med 22: 903, 2021.
4. Jandali D, Heilingoetter A, Ghai R, Jeffe J and Al-Khudari S: Large parotid gland lipoblastoma in a teenager. Front Pediatr 6: 50, 2018.
5. Besouw MT, Verlinde PF, Uyttebroeck AM and Renard MM: Lipoblastoma and lipoblastomatosis: Especially in children. Ned Tijdschr Geneeskd 155: A3467, 2011 (In Dutch).
6. McVay MR, Keller JE, Wagner CW, Jackson RJ and Smith SD: Surgical management of lipoblastoma. J Pediatr Surg 41: 1067-1071, 2006.
7. Voz ML, Mathys J, Hensen K, Pendeville H, Van Valckenborgh I, Van Huffel C, Chavez M, Van Damme B, De Moor B, Moreau Y and Van de Ven WJM: Microarray screening for target genes of the proto-oncogene PLAG1. Oncogene 23: 179-191, 2004.
8. Nitta Y, Miyachi M, Tomida A, Sugimoto Y, Nakagawa N, Yoshida H, Ouchi K, Tsuchiya K, Iehara T, Konishi E, *et al*: Identification of a novel BOC-PLAG1 fusion gene in a case of lipoblastoma. Biochem Biophys Res Commun 512: 49-52, 2019.
9. Juma AR, Damdimopoulou PE, Grommen SV, Van de Ven WJ and De Groef B: Emerging role of PLAG1 as a regulator of growth and reproduction. J Endocrinol 228: R45-R56, 2016.
10. Chen KS, Stroup EK, Budhipramono A, Rakheja D, Nichols-Vinueza D, Xu L, Stuart SH, Shukla AA, Fraire C, Mendell JT and Amatruda JF: Mutations in microrna processing genes in wilms tumors derepress the IGF2 regulator PLAG1. Genes Dev 32: 996-1007, 2018.
11. Patz M, Pallasch CP and Wendtner CM: Critical role of micrornas in chronic lymphocytic leukemia: Overexpression of the oncogene PLAG1 by deregulated mirnas. Leuk Lymphoma 51: 1379-1381, 2010.
12. Van Dyck F, Declercq J, Braem CV and Van de Ven WJ: PLAG1, the prototype of the plag gene family: Versatility in tumour development (Review). Int J Oncol 30: 765-774, 2007.
13. Kas K, Voz ML, Röijer E, Aström AK, Meyen E, Stenman G and Van de Ven WJ: Promoter swapping between the genes for a novel zinc finger protein and beta-catenin in pleiomorphic adenomas with t(3;8)(P21;Q12) translocations. Nat Genet 15: 170-174, 1997.
14. Hibbard MK, Kozakewich HP, Dal Cin P, Sciot R, Tan X, Xiao S and Fletcher JA: PLAG1 fusion oncogenes in lipoblastoma. Cancer Res 60: 4869-4872, 2000.
15. Matsuyama A, Hisaoka M and Hashimoto H: PLAG1 expression in mesenchymal tumors: An immunohistochemical study with special emphasis on the pathogenetical distinction between soft tissue myoepithelioma and pleomorphic adenoma of the salivary gland. Pathol Int 62: 1-7, 2012.
16. Andreasen S, von Holstein SL, Homøe P and Heegaard S: Recurrent rearrangements of the Plag1 and HMGA2 genes in lacrimal gland pleomorphic adenoma and carcinoma ex pleomorphic adenoma. Acta Ophthalmol 96: e768-e771, 2018.
17. Lopez-Nunez O, Alaggio R, Ranganathan S, Schmitt L, John I, Church AJ and Picarsic J: New molecular insights into the pathogenesis of lipoblastomas: Clinicopathologic, immunohistochemical, and molecular analysis in pediatric cases. Hum Pathol 104: 30-41, 2020.
18. Zhou J, Li X, Cai Y, Wang L and Yang SD: Undifferentiated myxoid lipoblastoma with PLAG1 gene rearrangement in infant. Pathol Res Pract 216: 152765, 2020.
19. Coffin CM, Lowichik A and Putnam A: Lipoblastoma (Lpb): A clinicopathologic and immunohistochemical analysis of 59 cases. Am J Surg Pathol 33: 1705-1712, 2009.
20. Kubota F, Matsuyama A, Shibuya R, Nakamoto M and Hisaoka M: Desmin-positivity in spindle cells: Under-recognized immunophenotype of lipoblastoma. Pathol Int 63: 353-357, 2013.
21. Sabah M, Cummins R, Leader M and Kay E: Aberrant expression of the Rb pathway proteins in soft tissue sarcomas. Appl Immunohistochem Mol Morphol 14: 397-403, 2006.
22. Louis-Brennetot C, Coindre JM, Ferreira C, Pérot G, Terrier P and Aurias AL: The CDKN2A/CDKN2B/CDK4/CCND1 pathway is pivotal in well-differentiated and dedifferentiated liposarcoma oncogenesis: An analysis of 104 tumors. Genes Chromosomes Cancer 50: 896-907, 2011.
23. He M, Aisner S, Benevenia J, Patterson F, Aviv H and Hameed M: P16 immunohistochemistry as an alternative marker to distinguish atypical lipomatous tumor from deep-seated lipoma. Appl Immunohistochem Mol Morphol 17: 51-56, 2009.
24. Gonzalez RS, McClain CM, Chamberlain BK, Coffin CM and Cates JM: Cyclin-dependent kinase inhibitor 2a (P16) distinguishes well-differentiated liposarcoma from lipoma. Histopathology 62: 1109-1111, 2013.
25. Abdul-Ghafar J, Ahmad Z, Tariq MU, Kayani N and Uddin N: Lipoblastoma: A clinicopathologic review of 23 cases from a major tertiary care center plus detailed review of literature. BMC Res Notes 11: 42, 2018.
26. de Saint Aubain Somerhausen N, Coindre JM, Debiec-Rychter M, Delplace J and Sciot R: Lipoblastoma in adolescents and young adults: Report of six cases with fish analysis. Histopathology 52: 294-298, 2008.
27. Creytens D: A contemporary review of myxoid adipocytic tumors. Semin Diagn Pathol 36: 129-141, 2019.
28. Yang X, Zhang L, Zhao W, Zhang Y and Yu J: Invasive angiomyxoma diagnosed by transvaginal ultrasound: A case report. Ann Palliat Med 10: 5870-5874, 2021.
29. Iwashita W, Kurabayashi A, Tanaka C, Naganuma S, Kawamura T, Aki F and Furihata M: Superficial angiomyxoma of the nipple in a Japanese woman: A case report and review of literature. Int J Surg Pathol 28: 683-687, 2020.
30. Al-Ibraheemi A, Martinez A, Weiss SW, Kozakewich HP, Perez-Atayde AR, Tran H, Parham DM, Sukov WR, Fritchie KJ and Folpe AL: Fibrous hamartoma of infancy: A clinicopathologic study of 145 cases, including 2 with sarcomatous features. Mod Pathol 30: 474-485, 2017.
31. Fritchie K, Wang L, Yin Z, Nakitandwe J, Hedges D, Horvai A, Mora JT, Folpe AL and Bahrami A: Lipoblastomas presenting in older children and adults: Analysis of 22 cases with identification of novel PLAG1 fusion partners. Mod Pathol 34: 584-591, 2021.

32. Mentzel T, Calonje E and Fletcher CD: Lipoblastoma and lipoblastomatosis: A clinicopathological study of 14 cases. Histopathology 23: 527-533, 1993.
33. Chung EB and Enzinger FM: Benign lipoblastomatosis. An analysis of 35 cases. Cancer 32: 482-492, 1973.
34. Collins MH and Chatten J: Lipoblastoma/lipoblastomatosis: A clinicopathologic study of 25 tumors. Am J Surg Pathol 21: 1131-1137, 1997.
35. Han JW, Kim H, Youn JK, Oh C, Jung SE, Park KW, Lee SC and Kim HY: Analysis of clinical features of lipoblastoma in children. Pediatr Hematol Oncol 34: 212-220, 2017.
36. Dao D, Najor AJ, Sun PY, Farrokhyar F, Moir CR and Ishitani MB: Follow-up outcomes of pediatric patients who underwent surgical resection for lipoblastomas or lipoblastomatosis: A single-institution experience with a systematic review and meta-analysis. Pediatr Surg Int 36: 341-355, 2020.
37. Yoshida H, Miyachi M, Ouchi K, Kuwahara Y, Tsuchiya K, Iehara T, Konishi E, Yanagisawa A and Hosoi H: Identification of COL3A1 and RAB2A as novel translocation partner genes of PLAG1 in lipoblastoma. Genes Chromosomes Cancer 53: 606-611, 2014.
38. Gisselsson D, Hibbard MK, Dal Cin P, Sciot R, His BL, Kozakewich HP and Fletcher JA: PLAG1 alterations in lipoblastoma: Involvement in varied mesenchymal cell types and evidence for alternative oncogenic mechanisms. Am J Pathol 159: 955-962, 2001.
39. Declercq J, Van Dyck F, Braem CV, Van Valckenborgh IC, Voz M, Wassef M, Schoonjans L, Van Damme B, Fiette L and Van de Ven WJM: Salivary gland tumors in transgenic mice with targeted plag1 proto-oncogene overexpression. Cancer Res 65: 4544-4553, 2005.
40. Asp J, Persson F, Kost-Alimova M and Stenman G: CHCHD7-PLAG1 and TCEA1-PLAG1 gene fusions resulting from cryptic, intrachromosomal 8q rearrangements in pleomorphic salivary gland adenomas. Genes Chromosomes Cancer 45: 820-828, 2006.
41. Matsuyama A, Hisaoka M, Nagao Y and Hashimoto H: Aberrant PLAG1 expression in pleomorphic adenomas of the salivary gland: A molecular genetic and immunohistochemical study. Virchows Arch 458: 583-592, 2011.
42. Asahina M, Saito T, Hayashi T, Fukumura Y, Mitani K and Yao T: Clinicopathological effect of PLAG1 fusion genes in pleomorphic adenoma and carcinoma ex pleomorphic adenoma with special emphasis on histological features. Histopathology 74: 514-525, 2019.
43. Klemke M, Müller MH, Wosniok W, Markowski DN, Nimzyk R, Helmke BM and Bullerdiek J: Correlated expression of HMGA2 and PLAG1 in thyroid tumors, uterine leiomyomas and experimental models. PLoS One 9: e88126, 2014.
44. Krsková L, Němečková T, Balko J, Brož P and Vícha A: Novel ZEB2-PLAG1 fusion gene identified by RNA sequencing in a case of lipoblastoma. Pediatr Blood Cancer 68: e28691, 2021.
45. Morerio C, Rapella A, Rosanda C, Tassano E, Gambini C, Romagnoli G and Panarello C: PLAG1-HAS2 fusion in lipoblastoma with masked 8q intrachromosomal rearrangement. Cancer Genet Cytogenet 156: 183-184, 2005.
46. Gerhard-Hartmann E, Vokuhl C, Roth S, Steinmüller T, Rosenfeldt M, Zamò A, Rosenwald A, Appenzeller S, Ernestus K and Maurus K: The histological and molecular spectrum of lipoblastoma: A case series with identification of three novel gene fusions by targeted rna-sequencing. Pathol Res Pract 226: 153591, 2021.
47. Warren M, Tiwari N, Sy S, Raca G, Schmidt RJ and Pawel B: Plag1 immunohistochemical staining is a surrogate marker for plag1 fusions in lipoblastomas. Pediatr Dev Pathol 25: 134-140, 2022.
48. Brčić I, Igrec J, Halbwedl I, Viertler C and Liegl-Atzwanger B: Expanding the spectrum of PLAG1-rearranged lipoblastomas arising in patients over 45, with identification of novel fusion partners. Mod Pathol 35: 283-285, 2022.
49. Chung CT, Antonescu CR, Dickson BC, Chami R, Marrano P, Fan R, Shago M, Hameed M and Thorner PS: Pediatric fibromyxoid soft tissue tumor with plag1 fusion: A novel entity? Genes Chromosomes Cancer 60: 263-271, 2021.
50. Warren M, Turpin BK, Mark M, Smolarek TA and Li X: Undifferentiated myxoid lipoblastoma with PLAG1-HAS2 fusion in an infant; morphologically mimicking primitive myxoid mesenchymal tumor of infancy (PMMTI)-diagnostic importance of cytogenetic and molecular testing and literature review. Cancer Genet 209: 21-29, 2016.
51. Morerio C, Nozza P, Tassano E, Rosanda C, Granata C, Conte M and Panarello C: Differential diagnosis of lipoma-like lipoblastoma. Pediatr Blood Cancer 52: 132-134, 2009.
52. Deen M, Ebrahim S, Schloff D and Mohamed AN: A novel PLAG1-RAD51L1 gene fusion resulting from a t(8;14)(Q12;Q24) in a case of lipoblastoma. Cancer Genet 206: 233-237, 2013.
53. Andersson MK, Åman P and Stenman G: IGF2/IGF1R signaling as a therapeutic target in MYB-positive adenoid cystic carcinomas and other fusion gene-driven tumors. Cells 8: 913, 2019.
54. Stenman G: Fusion oncogenes and tumor type specificity-insights from salivary gland tumors. Semin Cancer Biol 15: 224-235, 2005.
55. Alaggio R, Ninfo V, Rosolen A and Coffin CM: Primitive myxoid mesenchymal tumor of infancy: A clinicopathologic report of 6 cases. Am J Surg Pathol 30: 388-394, 2006.
56. Santiago T, Clay MR, Allen SJ and Orr BA: Recurrent bcor internal tandem duplication and BCOR or BCL6 expression distinguish primitive myxoid mesenchymal tumor of infancy from congenital infantile fibrosarcoma. Mod Pathol 30: 884-891, 2017.
57. Mirkovic J and Fletcher CD: Lipoblastoma-like tumor of the vulva: Further characterization in 8 new cases. Am J Surg Pathol 39: 1290-1295, 2015.
58. Coffin CM and Alaggio R: Adipose and myxoid tumors of childhood and adolescence. Pediatr Dev Pathol 15: 239-254, 2012.
59. Aust MC, Spies M, Kall S, Gohritz A, Boorboor P, Kolokythas P and Vogt PM: Lipomas after blunt soft tissue trauma: Are they real? Analysis of 31 Cases. Br J Dermatol 157: 92-99, 2007.
60. Alaggio R, Coffin CM, Weiss SW, Bridge JA, Issakov J, Oliveira AM and Folpe AL: Liposarcomas in young patients: A study of 82 cases occurring in patients younger than 22 years of age. Am J Surg Pathol 33: 645-658, 2009.
61. Ferreira J, Esteves G, Fonseca R, Martins C, André S and Lemos MM: Fine-needle aspiration of lipoblastoma: Cytological, molecular, and clinical features. Cancer Cytopathol 125: 934-939, 2017.
62. Jermendy G, Nádas J and Sápi Z: 'Lipoblastoma-like' lipoatrophy induced by human insulin: Morphological evidence for local dedifferentiation of adipocytes? Diabetologia 43: 955-956, 2000.
63. Cappellesso R, d'Amore ES, Dall'Igna P, Guzzardo V, Vassarotto E, Rugge M and Alaggio R: Immunohistochemical expression of P16 in lipoblastomas. Hum Pathol 47: 64-69, 2016.
64. Chen S, Deniz K, Sung YS, Zhang L, Dry S and Antonescu CR: Ewing sarcoma with ERG gene rearrangements: A molecular study focusing on the prevalence of fus-erg and common pitfalls in detecting EWSR1-ERG fusions by fish. Genes Chromosomes Cancer 55: 340-349, 2016.